JOURNAL OF MATERIALS SCIENCE **40** (2005) 4053–4059

Electrochemical characteristics of surface of titanium formed by electrolytic polishing and anodizing

CHIEN-CHON CHEN, JUNG-HSUAN CHEN, CHUEN-GUANG CHAO
Department of Materials Science and Engineering, National Chiao Tung University, Hsinchu, Taiwan 30050, Republic of China

WEN C. SAY
Department of Materials & Mineral Resources Engineering, National Taipei University of Technology, Taipei, Taiwan 106, Republic of China

A clear surface was polished using electrolytic polishing (EP). The mean roughness (Rz) of the polished surface was 1.966 nm, as measured by atomic force microscopy (AFM) over a 2×2 um^2 scan area. The various directions of the grains could be observed clearly following EP. The multiple beam interference effect generated various colors of the grains after anodic treatment at constant anodic voltage. A template with ordered nanochannel-array of anodic titanium oxide (ATO) was formed at 20 V. The template formed by self-assembly. The long-range ordered nanochannel had a thickness of 170 nm film, a pore size of 100 nm, an inter-pore distance of 120 nm, pore walls with a thickness of 25 nm , a pore density of 8×10^9 pores/cm^2, and a porosity of 68.2% , after anodizing for 90 s. When the applied voltage exceeded the breakdown voltage (90 V) of titania, the corrosion rate increased and the color of the titanium became as measured electrochemically by Tafel polarization and AC impedance methods, and observed by optical microscopy.

1. Introduction

The technique of anodizing titanium has been considered for many years to improve the surface properties of metal (including corrosion in reducing environments, wearing, galling, adherence of flue or paint) and to be useful in the development of new products, such as capacitors or templates [1–4]. In recent years, titanium oxides have found new areas of applications in converting solar energy, photocatalytic syntheses, photocatalytic degradation of certain organic pollutants and the electrolytic production of chlorine, among others [5–7]. The surfaces of Ti to be treated must be free of impurities must be planar so that electrolytic polishing can generate a bright and uniformly colored film adhered the Ti surface. Electrolytic polishing is extensively applied in research and industry [8–10]. Attaining high-quality surfaces by mechanical polishing is difficult even for the most competent metallographers. The idea of replacing at least the polishing stage of sample preparation with a relatively simple electrolytic treatment that can generate high-quality surfaces with good reproducibility, is highly appealing [11–13]

The surface of titanium metal is spontaneously covered with a 1–10 nm thick transparent film of titania on [14] if in air at room temperature. Additionally, increasing the thickness of the oxide film by anodizing causes it to become colored. The color of titanium oxide has been explained by multiple-beam interference theory [15]. Interference occurs between the beam reflected by the oxide surface and the beam that penetrates the oxide surface before being is reflected from the interface of the oxide surface and the titanium substrate. Hence, the non-uniformity of the oxide film on the specimen influences the interference colors. Restated, color is useful for identifying the thickness of titanium oxide. Moreover, the thickness of the oxide is determined by the applied voltage, with a growth constant of 2–3 nm/V [16]. Various colors are observed at constant voltage, but not if mechanical polishing is applied. The growing rates of films vary with the orientations of the surfaces of the grains, so the titanium surface has various colors at constant voltage. This technique is useful in identifying easily the specific orientation of a grain in a specimen by optical microscopy. A dense oxide film, such as anodic titanium oxide, is suitable to form a film of ordered nanochannel array. Anodic films with array ordered nanochannels are defined as films with nano-pores of sizes between 1 and 100 nm. They have attracted considerable attention because they have due to their special characteristics. Investigations have demonstrated that various characteristics, such as melting point, optical characteristics, electrical characteristics, and mechanical behaviors depend upon pore size [17–20]. Numerous nanochannel arrays of anodic

aluminum oxide (AAO) have been fabricated and studied; [11, 13, 22–29] however, few nanochannel arrays of ATO have been fabricated or studied [4, 39]. Titania is a useful catalytic and gas-sensing material. Titanium oxide thin films with nanoporous structures are desirable for use in these applications because due to their large surface areas and high reactivities. A dense ATO has been easily formed by anodizing titanium to promote anti-corrosion characteristics [16]. However, an array of nanoporous ATO cannot be easily formed because critical electrochemical conditions are required. In Dawei Gong's [4] work, the conditions used to fabricate nanochannel ATO on titanium foil were ananodizing voltage of 20 V for 20 min in 0.5% hydrofluoric at 18°C; however, when the anodizing time was under 20 minutes, sponge-like randomly porous structures were formed. In the experiment performed herein, the titanium substrate underwent electro-polishing and anodizing for 90 s, forming the nanochannel-array of ATO when the electrolyte was 1.2%HF + 10% H_2SO_4.

2. Experimental method

2.1. Electrolytic polishing

Highly pure titanium plates (99.995%) with an area of 2 cm × 2 cm were used. The specimen was annealed below the temperature of—phase transformation in an air furnace for one 1 h at 850°C, and was then abraded using1500-grit SiC paper. The electrolytic polishing conditions involved a platinum sheet (2 cm × 2 cm) as a cathode, titanium plates as an anode, 5% perchloric acid ($HClO_4$) + 53% ethylene glycol monobutylether ($HOCH_2CH_2OC_4H_9$) + 42% methanol (CH_3OH) as an electrolyte at 15°C, 52 V for one minute followed by 28 volts for 13 minutes, at a constant stirring rate of 200 rpm. Electrolytic polishing yielded a clear and planar surface on the titanium specimen.

2.2. Anodizing

The plane surface of titanium offers an area which anodizing can be studied. The anodizing conditions include a platinum sheet (2 cm × 2 cm) as a cathode, titanium plates as an anode and 10 vol.% sulfuric acid (H_2SO_4) as an electrolyte at 15°C. Constant voltages of 8, 15, 20, 30, 45, 60, 70, 80, 90 and 100 V were applied in the anodizing system, and the anodizing time at each constant voltage was five seconds. Anodizing yielded various colors of hypotitanous hydroxide ($Ti(OH)_4$) from the surface of the titanium. Additionally, 1.2 vol.%. hydrofluoric acid (HF) was added to the electrolyte of 10 vol.% H_2SO_4, and a long-range ordered nanochannel-array of ATO was obtained by applying for 90 seconds an anodizing voltage of 20 V.

2.3. Electrochemical measurement

A classical three-electrode electrochemical arrangement was used to test the electrochemical characteristics of the specimens [30–35]. The three-electrode electrochemical arrangement included a glass cylinder with a diameter of 1 cm fixed to the surface of the working electrode (titamium) via an O-ring, covering an area of 0.785 cm^2. The counter electrode was a platinum sheet (2 cm × 2 cm), and a saturated calomel electrode (SCE) was used for reference. The electrolyte was 0.9% NaCl solution. The electrochemical measurements of polarization curves were made using an EG&G Model 273A Potentiostat/Galvanostat. Electrochemical impedance spectroscopy (EIS) data were obtained using Solartron equipment—a 1286 electrochemical interface and a 1255 frequency response analyzer. This equipment covered a frequency range (of OR from) 1 MHz to 1 MHz, and the signal amplitude was 10 mV rms.

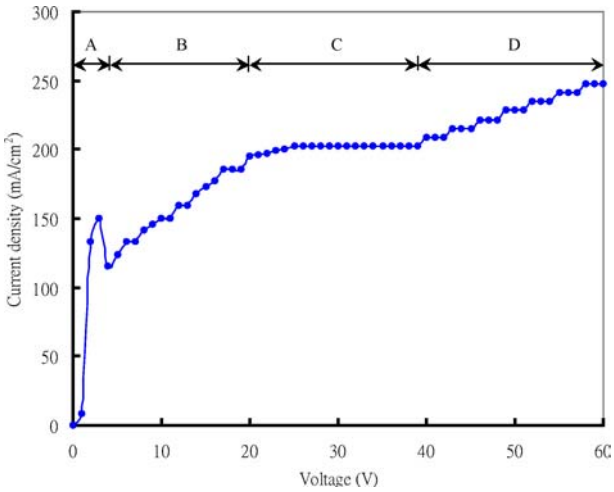

Figure 1 The electro-polishing curve of titanium.

3. Results and discussion

3.1. Morphology of electrolytically polished specimen

Fig. 1 shows the electrolytic polishing (EP) curve of titanium. Polishing is performed at the plateau (C); the oxide film is removed from the substrate at low voltage (A), etching is performed at (B), and gas is evolved and pitting occurs at high voltages (D). The appropriate polishing voltage for titanium was between 20 and 39 V; 28 V was chosen as the working voltage of anodization in this experiment. The EP process initially formed the black porous film, which had to be removed as quickly as possible. Two methods could be used to remove the film: the first is to increase the voltage; the second is to increase the rate of stirring. However, increasing the stirring rate can easily cause over polishing. In this study, the voltage was initially modified to 53 V for one minute and then the working voltage reduced to 28 V for 14 minutes. Hence, the cleaning and plating of the grains of α-phase Ti could be observed clearly. Fig. 2 displays a series of optical micrographs of EP obtained after various polishing times. EP was rough after it was abraded using 1500-grit SiC papers, as in (a). Polishing from 1 to 13 minutes, as shown in Figs b–h) did not suffice; the black porous film was removed first and the surface of the substrate was bright. The grain-boundary was observed but unclearly, after three minutes. Increasing polishing time caused the

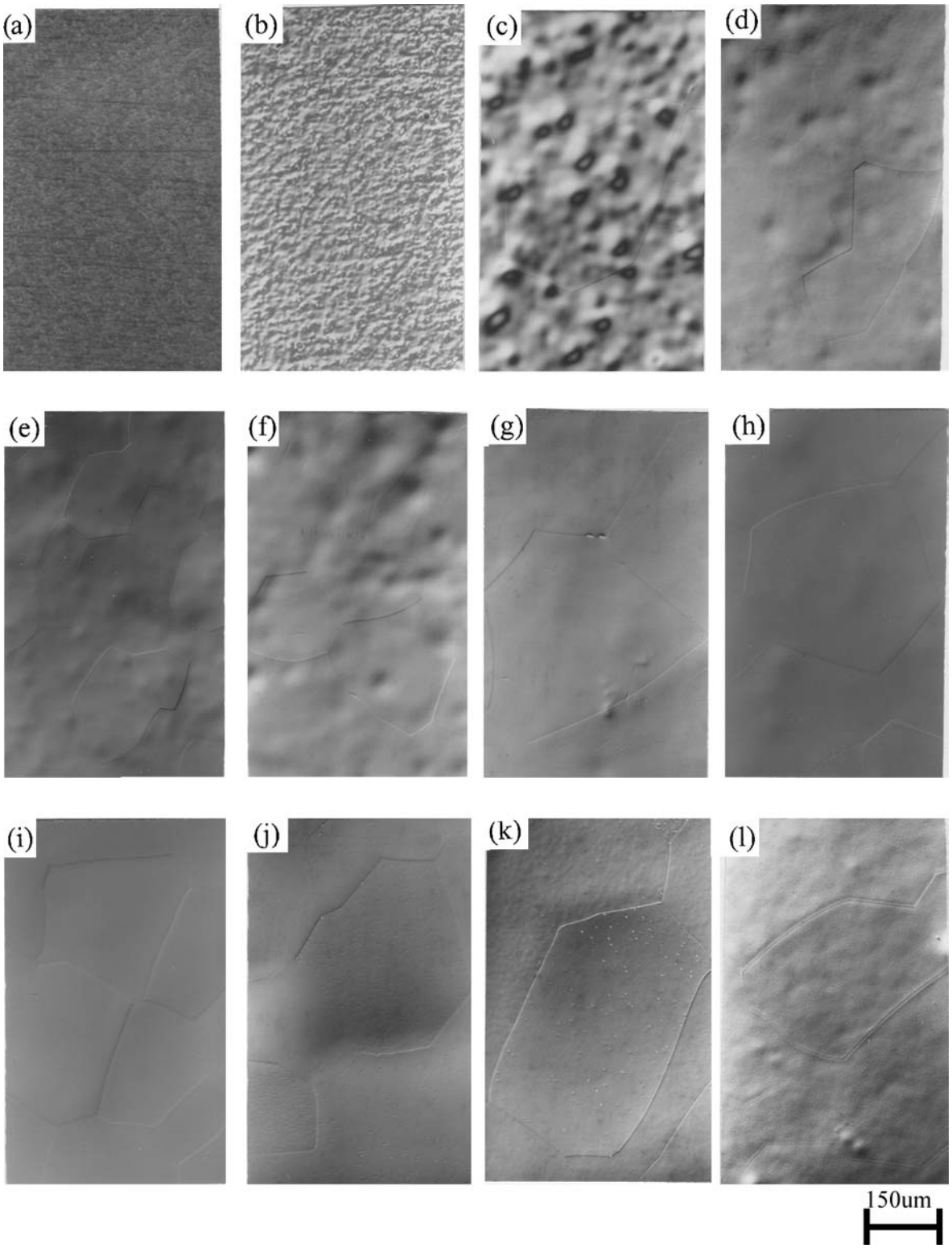

Figure 2 The optical micrographs of electro-polishing progress from 1 to 21 minutes on the titanium surface; (a) original titanium surface; (b)–(h) insufficient polishing, 1 to 13 minutes; (i) suitable polishing, 15 minutes; (j)–(k) excess polishing, 17 to 21 minutes.

grain-boundary to become distinct and the surface to become smooth. A favorable polishing time was 15 minutes, after which time the surface was flat, without scrapes with no pitting: as in Fig. i, in which the roughness of the polished surface, measured by AFM, was ∼1.966 nm over a 2 × 2 um scan area. When the polishing time exceeded 15 minutes, the grain-boundary was over-etched and the grain became pitted, as shown in Figs j–l.

3.2. Various colors of anodized electro-polished substrate

The literature [16] reveals that the applied voltage determines the thickness of oxide which grows at 2–3 nm/V. The color of the anodized titanium varies uniformly with the applied voltage, covering 6 V (light brown), 10 V (golden brown), 15 V (purple blue), 20 V (dark blue), 25 V (sky blue), 30 V (pale blue), 35 V ((steel blue), 40 V (light olive), 45 V (greenish

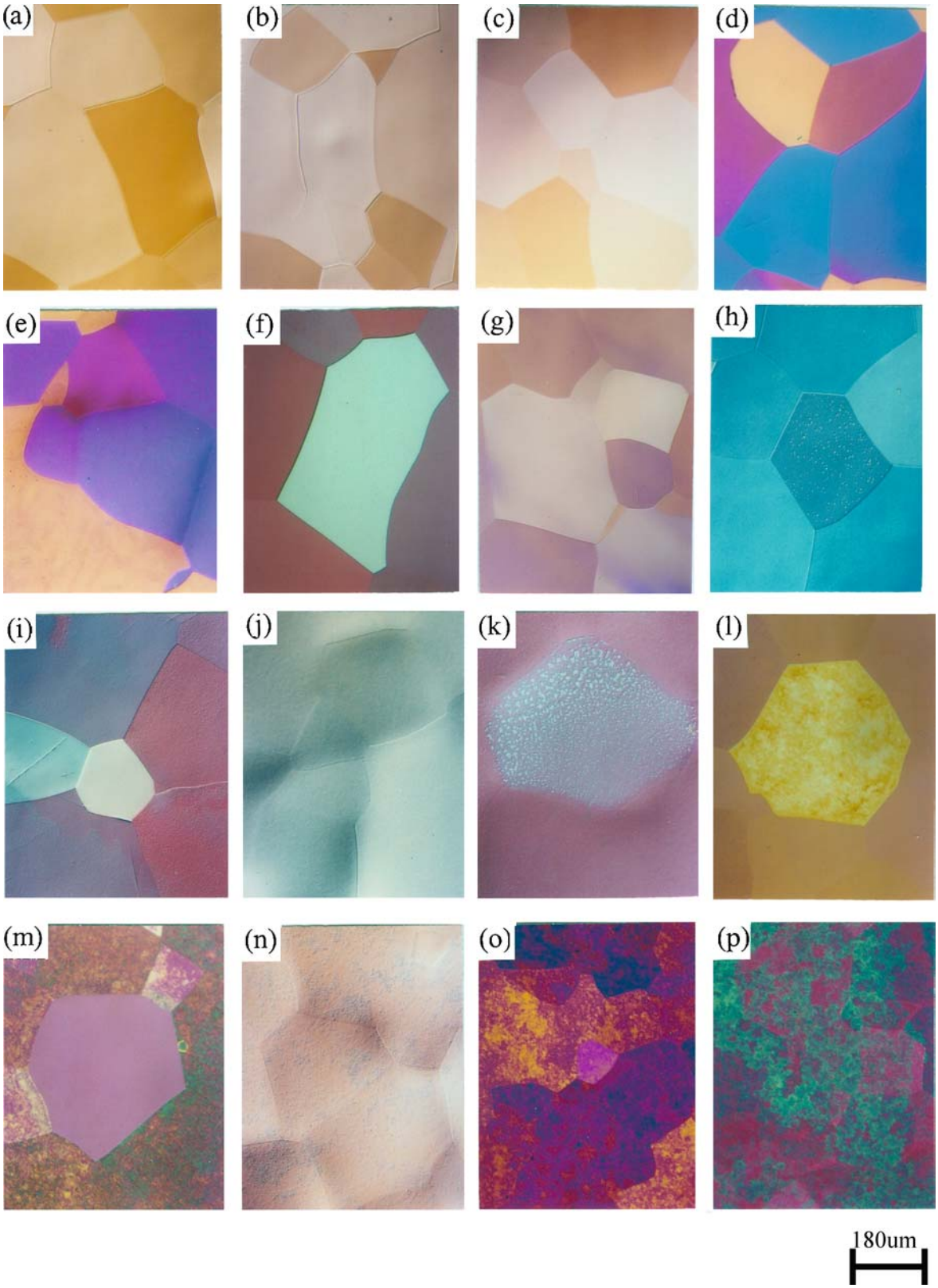

Figure 3 The optical micrographs of anodizing on the surface of titanium at different voltages; the films are porous-like when the applied voltage excess than 50 V; (a) 5 V, (b) 10 V, (c) 15 V, (d) 20 V, (e) 25 V, (f) 30 V, (g) 35 V, (h) 40 V, (i) 45 V, (j) 50 V, (k) 55 V, (l) 60 V, (m) 70 V, (n) 80 V, (o) 90 V, (p)100 V.

yellow), 50 V (lemon yellow), 55 V (golden), 60 V (pink), 75 V (blue) [16]. However, the EP surface of titanium does not vary uniformly with anodic treatment. Fig. 3 presents the different colors of the grains. When the applied voltage was under 40 V, the oxide film on the substrate was dense, as in Figs. 3a–h. Additionally, a large applied voltage generated a porous film on the specific grain, as in Figs 3i–l. When the voltage exceeded 90 V, a large quantity of gas escaped from the substrate, enabling the porous film to form on the substrate, as in Figs 3o and p. After EP, each grain at the surface could be observed clearly; additionally, the growth rate of the oxide films varied among the grains, so various colors were observed from the surface. The lack of uniformity

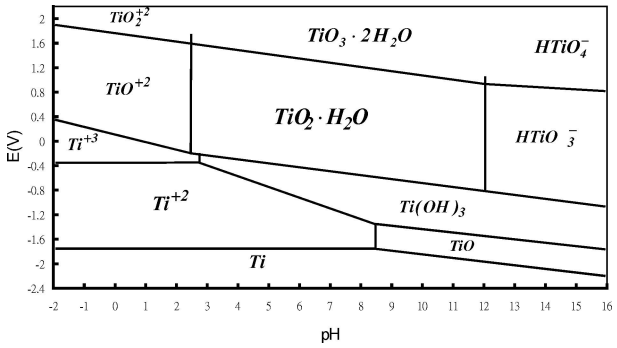

Figure 4 The Pourbaix diagram of titanium.

of the color of the grains was useful in identifying the grains and detecting changes to specific grains.

3.3. Pourbaix diagram of titanium

Immersing the titanium in electrolyte generated various substances. They included nine solids: titanium (Ti), titanium monoxide (TiO), hypotitanous hydroxide ($TiO{\cdot}H_2O$ or $Ti(OH)_2$), titanium sesquioxide (Ti_2O_3), titanium hydroxide ($Ti_2O_3{\cdot}H_2O$ or $Ti(OH)_3$), blue oxide (Ti_3O_5), titanium dioxide or rutile (TiO_2), hydrated dioxide ($TiO_2{\cdot}H_2O$ or $Ti(OH)_4$), hydrated peroxide ($TiO_3{\cdot}2H_2O$) and seven dissolved substances hypotitanous: ions (Ti^{+2}), titanous ions (Ti^{+3}), titanyl ions (TiO^{+2}), titanate ions ($HTiO_3^-$), pertitanyl ions (TiO_2^{+2}), acid pertitanate ions ($HTiO_4^-$) and pertitanate ions (TiO_4^{-2}) [36]. A complex reaction occurs among the 16 forms of titanium in aqueous solution. The Pourbaix diagram is useful in simplifying the complex reaction. The diagram is constructed by considering the Gibbs free energy and the Nernst equation. The titanium is not a noble metal. When an electrode potential of over -1.81 V (SHE) (which corresponds to an ion concentration of 10^{-6}) is applied, a passivating film of oxide is formed on its surface. Titanous: *check* ions, including Ti^{+2}, Ti^{+3}, TiO^{+2} and TiO_2^{+2} , are formed when the titanium is attacked by non-oxidizing strong acids (HF, HCl, $HClO_4$, . . .). TiO or $Ti(OH)_2$ and Ti_2O_3 or $Ti(OH)_3$ are unstable in water [36]. In the presence of acid solutions without an oxidizing agent, these ions dissolve with the evolution of hydrogen, generating and Ti^{+2} and Ti^{+3}. Ti_3O_5 is thermodynamically unstable with respect to TiO_2 and Ti_2O_3, and tends to decompose into a mixture of these two oxides. $TiO_3{\cdot}2H_2O$ is unstable in the presence of water and much more soluble than TiO_2 and $Ti(OH)_4$. It dissolves in acid solutions (with the formation of TiO_2^{+2} , and in alkaline solution with the formation $HTiO_3^-$, $HTiO_4^-$ and/or TiO_4^{-2}. TiO_2 or $Ti(OH)_4$ are more stable than all titanoul oxide. The oxide is quite soluble in strongly acidic solution, and is reduced to Ti^{+3} or TiO^{+2}.

The literature does not contain thermodynamic data on $HTiO_4^-$, TiO_4^{-2} or $TiO_3{\cdot}2H_2O$; however, the domains of these substances can be described on the Pourbaix diagram in Fig. 4, by considering the relationship among domains of TiO^{+2}, $Ti(OH)_2$ and $HTiO_3^-$. The oxide / hydrated oxides Ti_3O_5, $Ti(OH)_2$, $Ti(OH)_3$, $TiO_3{\cdot}2H_2O$, and $Ti(OH)_4$ in the solution are easy to dissolve, forming ion substances so the hydrated oxide $Ti(OH)_4$ is more stable than other hydrated oxides in the titanium Pourbaix system.

3.4. Forming array of nano-channels on ATO

A dense oxide film was formed on the titanium surface when the electrolyte was 10% H_2SO_4; however, an ordered nanochannel-array of ATO was obtained when 1.2% HF was added to the electrolyte. In addition, the color on the titanium surface changed from blue to almost transparent during the anodizing process, because a 68.2% porous film formed on the ATO, reducing the interference between the titanium and ATO. Numerous gases $TiF_{(g)}$, $TiF_{2(g)}$, $TiF_{3(g)}$, $TiF_{4(g)}$, $TiOF_{(g)}$ and $TiOF_{2(g)}$ are formed in the Ti-F-O system, according to the thermochemical data [37, 38]. When the titanium is anodized, the above gases and $H_{2(g)}$ escape from the titanium substance, leaving nanopores. Fig. 5a presents aplane view of an SEM micrograph image of ATO that was anodized in 1.2 vol.% HF + 10 vol. % H_2SO_4

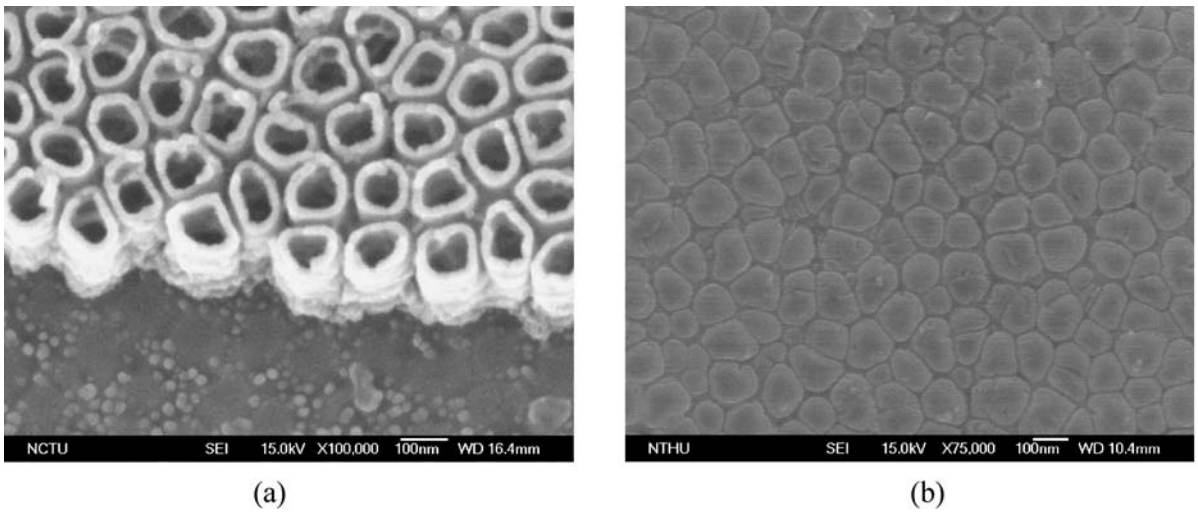

Figure 5 10% H_2SO_4 + 1.2% HF as the electrolyte, the ordered nanochannel array of ATO formed on the surface of titanium; (a) nanochannel of top view, (b) barrier layer of bottom view.

as an electrolyte at 25°C and 20 V for 90 seconds. The long-range ordered nano-channel had a 170 nm-thick film, pores with a diameter of 100 nm , an inter-pore distance of 120 nm, a 25nm-thick pore wall, a pore density of 8×10^{-9} pores/cm^2 and a porosity of 68.2%. Fig. 5b shows the barrier layer on the bottom of ATO.

The Pourbaix diagram of titanium shows that Ti dissolved as cations when the pH of the electrolyte wasunder 2.5, and the standard electrode potential exceeded −1.81 V(SHE). Applying a constant voltage of 20 V to the titanium effectively dissolved Ti according to $Ti \rightarrow Ti^{+2} \rightarrow TiO^{+2}$. TiO^{+2} combined easily with OH^- to form $TiO_2 \cdot H_2O$ or $Ti(OH)_4$ when the pH of the solution of titanly ions TiO^{+2} was increased to yield strongly acidic conditions. The enthalpy of formation of the precipitate of $Ti(OH)_4$ is unknown. It is an unstable substance, which changes gradually, by dehydration, into $TiO_2 \cdot H_2O$. A thin film of titania always forms on the surface of titanium after it is anodized. The thin film interference effect makes the thin TiO_2 film formed on the titanium surface easy to observe. In the experiment performed herein, when the electrolyte was 10% H_2SO_4 as, anodizing produced a dense dark blue oxidized layer on the titanium. The reaction equations were,

$$TiO^{+2} + 6OH^- + 2e^- \rightarrow Ti(OH)_4 + H_2 + 3O^{-2} \quad (1)$$

and,

$$TiO^{+2} + 2OH^- \rightarrow TiO_2 \cdot H_2O \quad (2)$$

3.5. Electrochemical test

A thin and dense layer of titanium oxide is always present on the surface of titanium, acting as an anti-corrosive film. The thickness of the film is proportional to the applied voltage and the rate of corrosion declines as the applied voltage increased; however, gas escapes and the titanium becomes heated when the applied voltage is excessive, increasing the corrosion rate. Table I presents the results of the electrochemical of Tafel polarization and the AC impedance test on the titanium oxide at various anodic voltages. The polarization of resistance were large, of the order of KΩ; the corrosion voltage was below 70 mV, the corrosion current density was of the order of nA/cm^2 scale, and the rate of corrosion was in the order of mmpy: . These results indicate the effectiveness of the anti-corrosion film on the surface of titanium after anodizing. Fig. 6 plots the curve of corrosion rate versus applied voltage; the corrosion rate declined as the voltage was reduced, especially below 20 V. When the voltage exceeded 90 V, the number of large pores in the film, and therefore the rate of corrosion, increased.

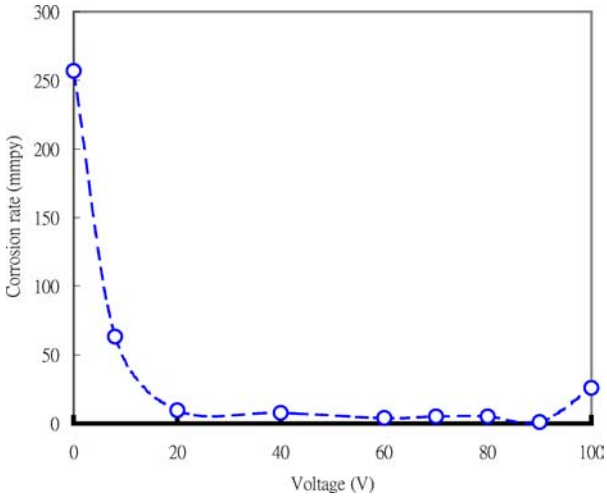

Figure 6 The curve of corrosion rate with anodic voltage.

In the AC impedance test, the resistances of the solution remained in the range 4 to 8 Ω , revealing that a static reaction occurred between buck and electrolyte. Additionally, the passive resistances increased with the applied voltage up to 90 V. When the applied voltage exceeded 90 V, the passive resistances declined as voltage further increased, which results agreed with those obtained in the Tafel polarization test. The density of the oxide film was evaluated by measuring passive capacitance. A denser oxide film has a lower passive capacitance. Table I lists the densities of the film with various anodic voltages up to 90 V. The results of the electrochemical test indicated that the ATO was stable below 90 V; however, when the applied voltage exceeded 90 V, a porous film was formed. Therefore, the polarization resistance, the corrosion voltage and the passive resistance all declined; the rate of corrosion and the passive capacitance increased.

TABLE I The results of electrochemical of Tafel polarization and AC impedance test on the ATO with varied anodic voltage in the 0.9% NaCl solution

Volts	0	10	20	40	60	70	80	90	100
				Tafel polarization					
Polarization resistance (R_P, K Ohm)	11.8	47.6	314.7	408.9	483.2	501.2	519.6	434.7	117.2
Corrosion voltage (E_{corr}, mV)	−62.45	−54.6	−60.87	−23.5	15.03	23.7	52.2	63.3	68.3
Corrosion current density (I_{corr}, nA/cm^2)	448.7	111.2	16.86	12.9	10.8	5.2	3.1	8.9	45.2
Corrosion rate (C. R., mmpy)	256.6	63.2	9.5	7.6	6.5	3.6	2.1	14.3	25.8
				AC. Impedance					
Solution resitance (R_{so}, Ohm)	4.2	6.2	8.1	5.8	4.5	6.5	4.8	4.6	6.4
Passive capacitance (C_{pf}, uF)	322	25.3	20.1	6.9	2.92	2.95	16.9	47.3	62.7
Passive resistance (R_{pf}, K ohm)	8.4	12.4	63.2	140.3	280	320.6	326.8	93.5	31.6

4. Conclusions

A uniformly colored anodic film was observed at constant voltage after mechanical polishing. The interference colors on the metal can be considered to identify quickly the thickness of the oxide below the breakdown voltage. Additionally, both of the optical micrograph and electrochemical testing revealed that the breakdown voltage of the ATO was 90 V. In this investigation, anodic films on the surface were not uniformly colored after the substrate was electro-polished. Anodic films on differently orientated grains were differently colored. The colors can be used to detect quickly the thickness of the oxide and the rate of growth rate on particular grains In addition, the appearance of various colors on the grains can be used to identify specific grains or detect changes in the thickness of the film on a specific grain. When 1.2% HF was added to the electrolyte at 20 V, the ordered nanochannel-array of ATO was formed. ATO had a film with a thickness of 170 nm, pores with diameters of 100 nm, an inter-pore distance of 120 nm, 25 nm-thick pore walls, a pore density of 8×10^9 pores/cm^2 and 68.2% porosity. Like AAO, ATO can be used in templates.

References

1. Y. T. SUL and C. B. JOHANSSON, *Med. Engg. Phys.* **23** (2001) 329.
2. H. HABAZAKI and M. UOZUMI, *Electrochem. Acta* **47** (2002) 3837.
3. F. SCHLOTTING and J. SCHRECKENBACH, *Appl. Surf.* **90** (1995) 129.
4. D. GONG and C. A. GRIMES, *J. Master. Res.* **16**(12) (2001) 3331.
5. R. WANG and K. HASHIMOTO, *Nature* **388**(31) (1997) 431.
6. M. GRATZEL, *Nature* **409**(1) (2001) 575.
7. T. OHTSUKA and T. OTSUKI, *J. Electroana. Chem.* **473** (1999) 272.
8. L. E. SAMUELS, *Metall.* **66**(396) (1962) 187.
9. L. HICKLING and J. K. HIGGINS, *Trans. Inst. Met. Finish.* **29** (1952) 274.
10. J. B. MATHIEU and H. J. MATHIEU, *J. Electrochem. Soc.* **125** (1978) 1039.
11. H. MASUDA and M. YOTSUYA, *Appl. Phys. Lett.* **78**(6) (2001) 826.
12. YING, United States Patent, Patent No.: 6231744, (2001).
13. R. C. SPOONER, *J. Electrochem. Soc.* **102**(4) (1955) 156.
14. J. L. DELPLANCKLE, *Degrez M, Surf. Technol.* **16** (1982) 153.
15. METALAST International, Inc., Metalast, METALAST Technical Bulletin, September **14** (2000) 1.
16. C. C. CHEN and HERHOLD A. B. *Science* **267** (1997) 398.
17. K. M. KULINOWSKI and P. JIANG, *Adv. Mater.* **12** (2000) 833.
18. S. H. TOBERT, *Phys. Rev. Lett* **76** (1996) 4384.
19. J. Z. JING and L.GERWARD, *J. Appl. Phys.* **87** (2000) 2658.
20. S. B.QADRI and J.YANG, *Appl. Phys. Lett.* **69** (1996) 2205.
21. G. E. THOMPSON and G. C. WOOD, *Nature*, **290** (1981) 230.
22. H. MASUDA and H. YAMADA, *Applied Physics Letters* **71**(19) (1997) 2772.
23. MASUDA, United States Patent, Patent No.: 6139713, (2000).
24. Miller, United States Patent, Patent No. : 5747180, (1998).
25. S. SETOH and A. MIYATA, *Sci. Pap. Inst. Phys. Chem. Res. Tokyo* (1932) 189.
26. AKAHORI, *J. Electronmicroscopy, Japan* (1962).
27. A. T. SHAWAQFEH and R. E. BALTUS, *J. Membrane Sci.* **157** (1999) 147.
28. G. PATERMARAKIS and K. MOUSSOUTZANIS, *Appl. Catal. Gen.* **180** (1999) 345.
29. I. S. MOLCHAN and N. V. GAPONENKO, *J. Alloys Comp.* **41** (2002) 251.
30. M. S. EL-BASIOUNY and A. A. MAZHAR, *Corrosion* **38**(5) (1982) 237.
31. D. C. SILVERMAN and J. E. CARRICO, *Corrosion* **44**(5) (1982) 280.
32. F. MANSFELD and H. SHIH, *ASTM STP* **1188** (1993) 37.
33. F. MANSFELD and W. J. LORENZ, *Corrosion Sci.* (1991) 581.
34. J. E. BAUERLE, *J. Phys. Chem. Solids* **30** (1969) 2657.
35. J. HITZIG, K. JUTTNER and W. J. LORENZ, *Corrosion Sci.* **24**(11/12) (1984) 945.
36. Marcel Pourbaix, NACE, USA, **213** (1974).
37. I. BARIN, Thermochemical Data of Pure Substances, Germany (1989).
38. M. W. CHASE, JR. and C. A. DAVIES, *J. Phys. Chem. Ref. Data* 1681 (1985).
39. R. BERANEK, H. HILDEBRAND and P. SHMUKI, *Electrochem. Solid-State Lett.* (2003) B12.

Received 19 January 2004
and accepted 11 March 2005